RSC Advances

PAPER

View Article Online
View Journal | View Issue

Cite this: *RSC Adv.*, 2024, **14**, 17866

Convenient synthesis and X-ray determination of 2-amino-6*H*-1,3,4-thiadiazin-3-ium bromides endowed with antiproliferative activity†

Hendawy N. Tawfeek,[ab] Alshaimaa Abdelmoez,[cd] Kholood A. Dahlous,[e] Bahaa G. M. Youssif, *[c] Stefan Bräse, *[f] Kari Rissanen, [g] Martin Nieger[h] and Essmat M. El-Sherief[a]

A new series of 1,3,4-thiadiazin-3-ium bromide derivatives **9a–g** were prepared as a six-member ring by interactions between 4-substituted thiosemicarbazides **8a–e** and α-halo ketones **2a**,**b**. The reaction was conducted using hydrazine-NH_2 and yielded a hexagonal shape. The structures of all obtained compounds have been verified using IR, NMR spectra, mass spectrometry, elemental analysis, and X-ray crystallography. The X-ray crystallographic analysis of compounds **9a** and **9b** has revealed that the salt is formed with the nitrogen atom N3 when the aromatic substituents **9a** and **9d** are present, but in the case of compounds **9b**, **9c**, **9e**, **9f**, and **9g** with the aliphatic substituent, the salt is formed outside the ring. Compounds **9a–g** were evaluated for antiproliferative activity as multitargeted inhibitors. Results revealed that targets **9a–g** displayed good antiproliferative activity, with GI_{50} ranging from 38 nM to 66 nM against a panel of four cancer cell lines compared to the reference Erlotinib (GI_{50} = 33 nM). Compounds **9a**, **9c**, and **9d** were the most potent antiproliferative derivatives, with GI_{50} values of 43, 38, and 47 nM, respectively. Compounds **9a**, **9c**, and **9d** were evaluated for their inhibitory activity against EGFR, $BRAF^{V600E}$, and VEGFR-2. The *in vitro* experiments demonstrated that the compounds being examined exhibit potent antiproliferative properties and have the potential to function as multitargeted inhibitors. In addition, the western blotting investigation demonstrated the inhibitory effects of **9c** on EGFR, $BRAF^{V600E}$, and VEGFR-2.

Received 3rd April 2024
Accepted 28th May 2024

DOI: 10.1039/d4ra02531h

rsc.li/rsc-advances

1. Introduction

Cancer remains a significant global problem. It is the second leading cause of death after heart problems.[1] There are currently more than 100 different forms of cancer, each necessitating a distinct diagnosis and therapy.[2] Many effective anti-cancer medicines, including standard chemotherapy drugs, suppress cell division and DNA replication. Nevertheless, many medications on the market are generic and often have common adverse effects.[3] Thus, searching for new lead structures and chemical components to develop effective, innovative anti-cancer drugs has become a top priority in medicinal chemistry, considering current cancer treatments' limitations and adverse effects.[4–6]

Anti-cancer medication discovery has heavily focused on developing treatments targeting a specific site with good efficacy and specificity. Clinical observations, such as identifying drug resistance in cancer treatment, have shown that focusing on one target may not always provide the intended biological outcome, even if the target is deactivated or suppressed.[7–9] The resistance develops due to the target's self-modification through mutation or the cancer cell's adoption of new routes for growth and multiplication.[10] Targeting a single oncoprotein has not led to successful treatment and may not be enough to establish long-lasting remission in patients.[11] Thus, adjusting the biological network is acknowledged to be advantageous.

There are currently two opposing methodologies for designing multi-targeting medicines. Combination medication therapy involves using numerous drugs that act on different

[a]*Chemistry Department, Faculty of Science, Minia University, El Minia, 61519 Egypt*
[b]*Unit of Occupational of Safety and Health, Administration Office of Minia University, El-Minia 61519, Egypt*
[c]*Pharmaceutical Organic Chemistry Department, Faculty of Pharmacy, Assiut University, Assiut 71526, Egypt. E-mail: bgyoussif2@gmail.com; bahaa.youssif@pharm.aun.edu.eg; Tel: +20-1098294419*
[d]*Department of Neurology, Ulm University, Ulm, Germany*
[e]*Department of Chemistry, College of Science, King Saud University, Riyadh 11451, Saudi Arabia*
[f]*Institute of Biological and Chemical Systems, IBCS-FMS, Karlsruhe Institute of Technology, 76131 Karlsruhe, Germany. E-mail: braese@kit.edu*
[g]*Department of Chemistry, University of Jyväskylä, PO Box 35, 40014 Jyväskylä, Finland*
[h]*Department of Chemistry, University of Helsinki, PO Box 55, A. I. Virtasen Aukio 1, 00014 Helsinki, Finland*

† Electronic supplementary information (ESI) available. CCDC 2329624 (**9a**) and 2329625 (**9b**). For ESI and crystallographic data in CIF or other electronic format see DOI: **https://doi.org/10.1039/d4ra02531h**

targets to provide an additive or synergistic impact. Combination therapies have shown success in treating metastatic melanoma with BRAF mutations.[12,13] The FDA has approved the combination of dabrafenib (BRAF inhibitor) and trametinib (MEK inhibitor) based on preclinical evidence of increased apoptosis and delayed resistance to serine/threonine-protein kinase B-Raf.[14,15] Phase III clinical trials have shown good results for combination therapy using RAF inhibitor (vemurafenib) and MEK inhibitor (cobimetinib) in treating BRAF mutant melanoma.[16] Another successful example of combination therapy involves utilizing palbociclib and letrozole to treat advanced breast cancer.[17]

The second approach is to identify and develop medicines that target numerous oncogenic pathways simultaneously. Multi-targeting therapies entail the discovery of a single agent capable of simultaneously acting on two or more targets.[18–20] The US Food and Drug Administration (FDA) has approved Lenvima (Lenvatinib) as a receptor tyrosine kinase inhibitor that blocks the kinase activities of vascular endothelial growth factor (VEGF) receptors VEGFR1, VEGFR2, and VEGFR3.[21] Cabozantinib, known as cabometyx, is an FDA-approved small molecule inhibitor targeting the tyrosine kinases c-Met and VEGFR-2. It has effectively reduced tumor growth, metastasis, and angiogenesis.[21]

Nitrogen and sulfur-containing compounds are commonly used as the basis for various biological components in medicinal chemistry.[22–24] Thiadiazine-based compounds have garnered considerable attention for their broad applicability as physiologically active molecules.[25,26] Thiadiazine derivatives have shown significant cytotoxic effects on cancer cell lines by disrupting DNA synthesis, causing cell cycle arrest, inhibiting tumor cell invasion and migration, triggering apoptosis through the mitochondrial pathway, and blocking various nuclear enzymes.[27–31]

Ragab *et al.*[27] described the design, synthesis, and biological testing of novel 1,3,4-thiadiazine-based derivatives as potential anti-cancer agents against non-small cell lung cancer (NSCLC) cells. The most effective compounds were chosen for further study as multitargeted inhibitors of VEGFR-2, $BRAF^{V600E}$, and matrix metalloproteinase 9 (MMP9). Compound **I** (Fig. 1) showed the most promising results among the compounds tested. It demonstrated inhibitory activity against VEGFR-2, similar to Sorafenib, with an IC_{50} value of 0.11 ± 0.01 μM. It also exhibited the most potent suppression of $BRAF^{V600E}$ activity, with an IC_{50} value of 0.178 ± 0.004 μM, and MMP9 inhibition, with an IC_{50} value of 0.08 ± 0.004 μM.

Another study explored the synthesis of some novel anticancer agents derived from triazolothiadiazine. When tested against a panel of NCI-60 cancer cell lines.[29] Compound **II** (Fig. 1) showed a potential antiproliferative effect. Compound **II** was evaluated against 16 kinases to determine its antiproliferative mechanism. The study significantly suppressed EGFR, VEGFR-2, CDK-2, and GSK-3β. Furthermore, compound **II** increased the amount of active caspase-3, causing cell cycle arrest at the G2-M phase with apoptotic action.

On the other hand, phenacyl bromides, also known as α-halo ketones and primary alkyl halides, play a crucial role in chemical synthesis. They serve as crucial building blocks in heterocyclic constructions as a vital intermediate for synthesizing various bioactive chemicals and natural products.[32] Also, thiosemicarbazides are a vital class of organic compounds that operate as the backbone of a range of heterocyclic compounds of considerable interest in medical and industrial uses.[33,34] Additionally, interactions with phenacyl bromides revealed that thiosemicarbazides have several active centers.[35] Busby and Domincy were the first to investigate the behavior of 4-substituted thiosemicarbazides toward haloketones, obtaining 2-amino-1,3,4-thiadiazines.[36] Pfeiffer *et al.* synthesized 1,3,4-thiadiazines by combining α-halo ketones and 1,2,4-trialkyl thiosemicarbazides. The structure of the thiadiazines was confirmed through desulfurization with acetic acid.[37] Several methods synthesized 1,3,4-thiadiazine, including interactions

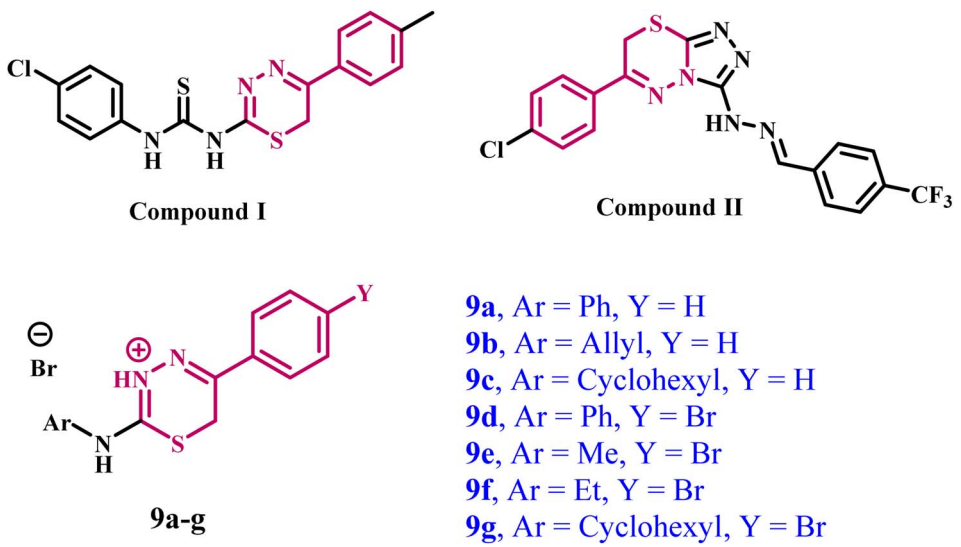

Fig. 1 Structures of some reported 1,3,4-thiadiazine-based multitargeted anti-cancer agents and target compounds **9a–g**.

between thiosemicarbazides and α-halo ketones in different solvents.[38,39] However, Aly *et al.*[40] demonstrated the one-pot synthesis of 2-ylidenehydrazonothiazoles from the reaction of 4-substituted thiosemicarbazides, ketones, and phenacyl bromide, and they proposed that the product was obtained through the formation of the hydrazinylthiazole intermediate, which contradicted the findings of Pfeiffer *et al.*[41]

In light of the previous data on the multitargeted inhibitory action of 1,3,4-thiadiazine derivatives and our ongoing efforts to develop multitargeted anti-cancer agents,[6,7,19,42–44] this investigation focuses on the synthesis of new 1,3,4-thiadiazine derivatives (**9a–g**, Fig. 1) as multitargeted antiproliferative agents.

2. Experiments

2.1. Chemistry

2.1.1 General details: see Appendix A. 4-Substituted thiosemicarbazides **8a–e**[45] were prepared according to published literature, and 2-bromo-1-phenylethanone (**2a**), 2-bromo-1-(4-bromophenyl)ethanone (**2b**) were used as purchased from Merck.

2.1.2. General procedure for the synthesis of 2-substituted amino-1,3,4-thiadiazin-3-ium bromide derivatives (9a–g). In a conical flask, mix 1 mmol of 4-substituted thiosemicarbazides **8a–e** with 199 mg of 2-bromo-1-phenylethanone (1 mmol, **2a**) or 278 mg of 2-bromo-1-(4-bromophenyl)ethanone (1 mmol, **2b**) in 30 ml ethanol at low temperature. The reaction mixtures were stirred magnetically at room temperature for 1–2 hours. Then, the resulting solid was filtered off and washed with ethanol three times, dried well, and recrystallized from hot ethanol to afford the thiadiazinium bromides **9a–g** in excellent yields.

2.1.3. 5-Phenyl-2-(phenylamino)-6*H*-1,3,4-thiadiazin-3-ium bromide (9a). Colorless crystals (95%, 0.329 g), m.p. = 197–198 °C. IR (KBr, cm^{-1}): 3164 (NH), 3015 (Ar-CH), 2988 (ali-CH), 1617 (C=N), 1594 (C=C) cm^{-1}. ^{1}H NMR (300 MHz, $CDCl_3$): δ_H = 3.91 (s, 2H, CH_2), 7.35–7.48 (m, 6H, Ar-H), 7.88–7.94 (m, 2H, Ar-H), 8.01–8.04 (m, 2H, Ar-H), 9.45 (bs, 1H, exocyclic-NH), 12.85 (bs, 1H, cyclic-NH^+) ppm. ^{13}C NMR (75 MHz, DMSO-d_6): δ_c = 23.26 (CH_2), 123.84, 126.01, 127.67, 128.80, 129.46, 130.03 (Ar-CH), 132.94, 139.15 (Ar–C), 144.32 (thiadiazine-C5), 150.71 (thiadiazine-C2) ppm. MS (70 eV) *m*/*z* (%): 347 (M^+, 9), 267 (100), 155 (10), 119 (5). Anal. calcd for $C_{15}H_{14}BrN_3S$ (348.26) calcd: C, 51.73; H, 4.05; N, 12.07; S, 9.21. Found: C, 51.81; H, 3.99; N, 12.13; S, 9.28.

2.1.4. (*Z*)-*N*-(5-Phenyl-3,6-dihydro-2*H*-1,3,4-thiadiazin-2-ylidene)prop-2-en-1-aminium bromide (9b). Yellow crystals (91%, 0.287 g), m.p. = 224–226 °C. IR (KBr, cm^{-1}). ^{1}H NMR (300 MHz, $CDCl_3$): δ_H = 4.01–4.04 (m, 2H, Allyl-CH_2), 4.10 (s, 2H, CH_2), 5.23–5.34 (m, 2H, Allyl-CH_2=), 5.72–5.83 (m, 1H, Allyl-CH=), 7.33–7.44 (m, 3H, Ar-H), 7.72–7.79 (m, 2H, Ar-H), 10.62 (bs, 1H, exocyclic-NH^+), 12.98 (bs, 1H, cyclic-NH) ppm. ^{13}C NMR (75 MHz, $CDCl_3$): δ_c = 22.99 (CH_2), 48.01 (CH_2-Allyl), 119.91 (Allyl-CH_2=), 127.01, 129.02, 130.17, 131.71 (Ar-CH), 132.18 (Ar-C), 149.36 (C5), 166.75 (C2) ppm. MS (70 eV) *m*/*z* (%): 311 (M^+, 15), 283 (28), 199 (54), 189 (10), 119 (33), 102 (100). Anal. calcd for $C_{12}H_{14}BrN_3S$ (311.23) calcd: C, 46.16; H, 4.52; N, 13.46; S, 10.27. Found: C, 46.23; H, 4.59; N, 13.39; S, 10.30.

2.1.5. (*Z*)-*N*-(5-Phenyl-3,6-dihydro-2*H*-1,3,4-thiadiazin-2-ylidene) cyclohexanaminium bromide (9c). Yellow crystals (86%, 0.300 g), m.p. = 217–219 °C. IR (KBr, cm^{-1}): 3158 (NH), 3106, 3027 (Ar-CH), 2992, 2917 (ali-CH), 1613, 1581 (C=N), 1538, 1445 (C=C) cm^{-1}. ^{1}H NMR (300 MHz, $CDCl_3$): δ_H = 125–1.33, 1.36–1.69, 2.01–2.04 (m, 10H, cyclohexyl-CH_2), 3.02–3.09 (m, 1H, cyclohexyl-CH), 3.55 (s, 2H, CH_2), 7.33–7.37 (m, 3H, Ar-H), 7.80–7.82 (m, 2H, Ar-H), 10.20 (bs, 1H, exocyclic-NH^+), 11.84 (bs, 1H, cyclic-NH) ppm. ^{13}C NMR (75 MHz, $CDCl_3$): δ_c = 22.46 (CH_2), 24.54, 25.23, 33.30 (cyclohexyl-CH_2), 52.98 (cyclohexyl-CH), 126.34, 128.42, 129.50 (Ar-CH), 135.31 (Ar-C), 147.38 (C5), 166.85 (C2) ppm. MS (70 eV) *m*/*z* (%): 353 (M^+, 3), 274 (M^+-HBr, 100), 192 (7), 133 (3), 104 ($[PhCN]^+$, 4). Anal. calcd for $C_{15}H_{20}BrN_3S$ (354.31) calcd: C, 50.85; H, 5.69; N, 11.86; S, 9.05. Found: C, 50.78; H, 5.63; N, 11.90; S, 9.11.

2.1.6. 5-(4-Bromophenyl)-2-(phenylamino)-6*H*-1,3,4-thiadiazin-3-ium bromide (9d). Yellow crystals (87%, 0.371 g), m.p. = 185–186 °C. ^{1}H NMR (300 MHz, DMSO-d_6): δ_H = 3.96 (s, 2H, CH_2), 7.19–7.39 (m, 3H, Ar-H), 7.61–7.68 (m, 2H, Ar-H), 7.71–7.76 (m, 2H, Ar-H), 7.78–7.89 (m, 2H, Ar-H), 10.48 (bs, 1H, exocyclic-NH), 12.64 (bs, 1H, cyclic-NH^+) ppm. ^{13}C NMR (75 MHz, DMSO-d_6): δ_c = 40.33 (CH_2), 124.39, 125.81, 128.27, 129.30, 131.47 (Ar-CH), 123.64, 135.13, 138.55 (Ar-C), 146.12 (C5), 158.63 (C2) ppm. MS (70 eV) *m*/*z* (%): 347 (M^+, 9), 267 (100), 155 (10), 119 (5). Anal. calcd for $C_{15}H_{13}Br_2N_3S$ (427.16) calcd: C, 42.81; H, 3.07; N, 9.84; S, 7.51. Found: C, 42.87; H, 3.00; N, 9.78; S, 7.47.

2.1.7. (*Z*)-*N*-(5-(4-Bromophenyl)-3,6-dihydro-2*H*-1,3,4-thiadiazin-2-ylidene) methanaminium bromide (9e). Yellow crystals (78%, 0.295 g), m.p. = 211–213 °C, ^{1}H NMR (300 MHz, DMSO-d_6): δ_H = 2.69 (s, 2H, CH_3), 4.09 (s, 3H, CH_2), 7.62–7.65 (dd, 2H, J = 6.6, Ar-H), 7.70–7.73 (dd, 2H, J = 6.6 Ar-H), 11.78 (bs, 1H, exocyclic-NH^+), 12.23 (bs, 1H, cyclic-NH) ppm. ^{13}C NMR (75 MHz, DMSO-d_6): δ_c = 30.18 (CH_3), 48.66 (CH_2), 129.17, 131.40 (Ar-CH), 123.33, 137.17 (Ar-C), 145.66 (C5), 172.76 (C2) ppm. Anal. calcd for $C_{10}H_{11}Br_2N_3S$ (365.09) calcd: C, 32.90; H, 3.04; N, 11.51; S, 8.78. Found: C, 32.83; H, 3.08; N, 11.46; S, 8.80.

2.1.8. (*Z*)-*N*-(5-(4-Bromophenyl)-3,6-dihydro-2*H*-1,3,4-thiadiazin-2-ylidene)ethan aminium bromide (9f). Yellow crystals (78%, 0.295 g), m.p. = 190–192 °C, ^{1}H NMR (300 MHz, DMSO-d_6): δ_H = 1.38–1.79 (t, 3H, J = 7.5, CH_3–CH_2), 3.55–3.60 (q, 2H, J = 7.5, CH_2–CH_3) 3.65 (s, 1H, cyclic-CH_2), 7.62–7.65 (dd, 2H, J = 8.1, Ar-H), 7.71–7.74 (dd, 2H, J = 8.4 Ar-H), 11.73 (bs, 1H, exocyclic-NH^+), 12.31 (bs, 1H, cyclic-NH) ppm. ^{13}C NMR (75 MHz, $CDCl_3$): δ_c = 14.29 (CH_3CH_2–), 38.66 (CH_2–CH_3), 40.33 (CH_2), 129.00, 131.14 (Ar-CH), 122.74, 135.79 (Ar-C), 147.24 (C5), 165.64 (C2) ppm. Anal. calcd for $C_{11}H_{13}Br_2N_3S$ (379.11) calcd: C, 34.85; H, 3.46; N, 11.08; S, 8.46. Found: C, 34.90; H, 3.41; N, 11.12; S, 8.43.

2.1.9. (*Z*)-*N*-(5-(4-Bromophenyl)-3,6-dihydro-2*H*-1,3,4-thiadiazin-2-ylidene) cyclohexanaminium bromide (9g). Yellow crystals (81%, 0.350 g), m.p. = 203–205 °C ^{1}H NMR (300 MHz, $CDCl_3$): δ_H = 1.17–1.30, 1.38–1.79 (m, 8H, cyclohexyl-CH_2), 2.04–2.14 (m, 3H, cyclohexyl-CH_2 and cyclohexyl-CH), 4.29 (s, 2H, CH_2), 7.45–7.48 (dd, 2H, J = 8.4, Ar-H), 7.49–7.58 (dd, 2H, J =

8.4, Ar–H), 10.89 (bs, 1H, exocyclic-NH^+), 12.65 (bs, 1H, cyclic-NH) ppm. ^{13}C NMR (75 MHz, $CDCl_3$): δ_c = 24.74 (CH_2), 25.03, 25.22, 32.51 (cyclohexyl-CH_2), 52.40 (cyclohexyl-CH), 128.05, 130.24 (Ar-CH), 132.05, 135.62 (Ar-C), 158.20 (C5), 174.57 (C2) ppm. Anal. calcd for $C_{15}H_{19}Br_2N_3S$ (433.21) calcd: C, 41.59; H, 4.42; N, 9.70; S, 7.40. Found: C, 41.63; H, 4.43; N, 9.62; S, 7.51.

2.2. Crystal X-ray structure determination of 9a and 9b

The single-crystal X-ray diffraction studies were carried out on a Rigaku XtaLAB Synergy R diffractometer with HyPix-Arc 100 detector at 133(2) K using Cu-Kα radiation (**9a**, λ = 1.54178 Å, PhotonJet R rotating anode generator) or a Bruker D8 Venture diffractometer with a PhotonII detector at 173(2) K using Cu-Kα radiation (**9b**, λ = 1.54178 Å). Dual space methods (SHELXT) [G. M. Sheldrick, *Acta Crystallogr.*, 2015, **A71**, 3–8] were used for structure solution, and refinement was carried out using SHELXL-2014 (full-matrix least-squares on F^2) [G. M. Sheldrick, *Acta Crystallogr.*, 2015, **C71**, 3–8]. Hydrogen atoms were localized by difference electron density determination and refined using a riding model. An extinction correction and a semi-empirical absorption correction were applied.

9a: colourless crystals, $C_{15}H_{14}N_3S\cdots Br$, M_r = 348.26, crystal size 0.18 × 0.14 × 0.13 mm, monoclinic, space group $P2_1/n$ (no. 14), a = 8.9077(1) Å, b = 9.1847(1) Å, c = 18.1367(2) Å, β = 93.364(1)°, V = 1481.29(3) Å^3, Z = 4, ρ = 1.562 mg m^3, μ(Cu-K_α) = 5.04 mm^{-1}, $F(000)$ = 704, T = 133 K, $2\theta_{max}$ = 158.6°, 16 484

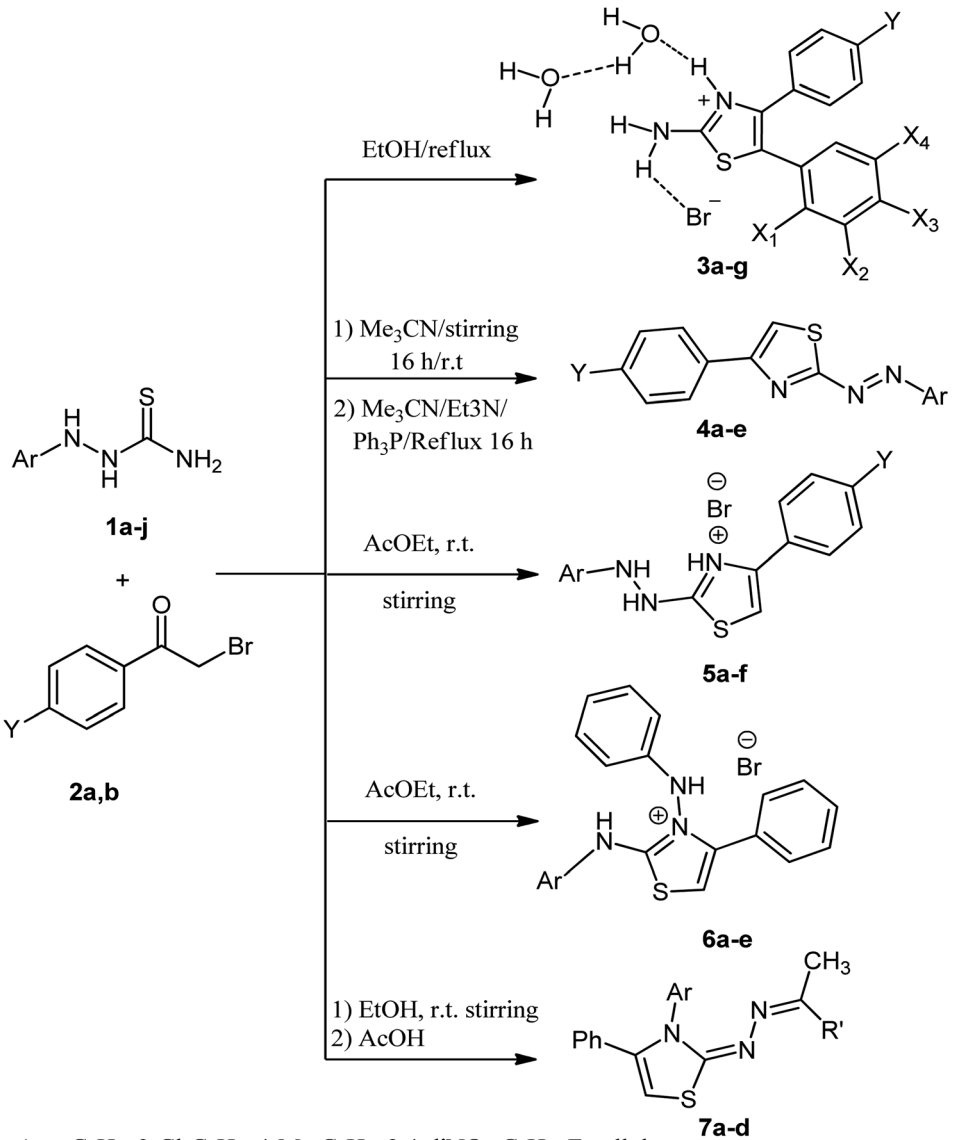

Ar = C_6H_5, 3-Cl-C_6H_4, 4-Me-C_6H_4, 2,4-diNO_2-C_6H_3, Et, allyl, 4-Me-C_6H_4-SO_2-, benzyl, cyclohexyl, Me

Y = H, Br

X = H, NH_2, Cl, Me, SO_2NH_2, NO_2

Scheme 1 Reactivity of substituted thiosemicarbazides toward phenacyl bromide.

reflections, of which 3177 were independent ($R_{int} = 0.016$), 188 parameters, 2 restraints, $R_1 = 0.020$ (for 3161 $I > 2\sigma(I)$), wR_2 = 0.051 (all data), $S = 1.09$, largest diff. peak/hole = 0.33/−0.31 e Å^{-3}.

9b: yellow crystals, $C_{12}H_{14}N_3S\cdots Br$, $M_r = 312.23$, crystal size 0.14 × 0.25 × 0.20 mm, orthorhombic, space group *Pbca* (no. 61), $a = 7.4414(3)$ Å, $b = 18.2272(7)$ Å, $c = 19.6573(7)$ Å, $V = 2666.24(18)$ Å^3, $Z = 8$, $\rho = 1.556$ mg m^3, μ(Cu-K$_\alpha$) = 5.51 mm^{-1}, $F(000) = 1264$, $T = 173$ K, $2\theta_{max} = 144.2°$, 19 426 reflections, of which 2613 were independent ($R_{int} = 0.033$), 161 parameters, 2 restraints, $R_1 = 0.022$ (for 2558 $I > 2\sigma(I)$), w$R_2 = 0.056$ (all data), $S = 1.05$, largest diff. peak/hole = 0.28/−0.25 e Å^{-3}.

CCDC 2329624 (**9a**) and 2329625 (**9b**) contain the supplementary crystallographic data for this paper.

2.3. Biology

2.3.1. Cell viability assay. The human mammary gland epithelial (MCF-10A) normal cell line was used to investigate the viability effect of new targets **9a–g** on viability.[46,47] Refer to Appendix A for more details.

2.3.2. Antiproliferative assay. The MTT assay[5,48] was used to investigate the antiproliferative efficacy of targets **9a–g** against four human cancer cell lines: lung cancer (A-549) cell line, colon cancer (HT-29), pancreatic cancer (Panc-1) cell line, and breast cancer (MCF-7) cell line. Erlotinib was used as a reference. See Appendix A for more details.

2.3.3. EGFR inhibitory assay. The EGFR-TK test[49,50] was performed to assess the inhibitory strength of the most potent antiproliferative derivatives **9a**, **9c**, and **9d** against EGFR. See Appendix A for more information.

2.3.4. BRAF^{V600E} inhibitory assay. *In vitro* testing assessed the anti-BRAF^{V600E} activity of compounds **9a**, **9c**, and **9d**.[51,52] Refer to Appendix A.

2.3.5. VEGFR-2 assay. The inhibitory potency of compounds **9a**, **9c**, and **9d** against VEGFR-2 was assessed using kinase-glo-luminescent kinase assays,[53] with Sorafenib as the reference drug. See Appendix A for more details.

2.4. Western blotting assay

The western blotting analysis[54] aids in elucidating the probable mechanisms behind the observed antiproliferative activity of **9c**. Appendix A contain all details related to the assay methodology.

3. Results and discussion

3.1. Chemistry

According to prior research and our own,[35,41,55] the interaction between thiosemicarbazides and phenacyl bromides is principally determined by the reaction conditions, substituted position, and solvent employed, as seen in Scheme 1. All obtained compounds were confirmed by X-ray crystallographic determination.

Based on previous research and our interest in phenacyl bromide reactions, we found that the reaction between phenacyl bromide and 1/or 2-substituted thiosemicarbazides results in the formation of a five-membered ring (thiazole-ring). In the current study, the reaction of phenacyl bromides (**2a,b**) with 4-substituted thiosemicarbazides (**8a–e**) in absolute ethanol with no catalyst resulted in the synthesis of 2-substituted amino-1,3,4-thiadiazinium bromide derivatives (**9a–g**). This reaction formed six-membered rings, as shown in Scheme 2. In this context, the differential behavior of 4-substituted thiosemicarbazides **8a–e** *versus* 1/or 2-substituted thiosemicarbazides influences hexagonal ring formation. This mismatch explains the observed differential in nucleophilicity of the NH_2 group, which first reacts with the carbonyl group before cycling through the SH group. This effect compelled the reaction to yield thiadiazine as six-membered ring, rather than the five-membered ring characteristic of thiazole.

All obtained compounds are recrystallized from ethanol, and their structures were confirmed with advanced spectroscopic analysis tools such as IR, mass, and NMR spectrum (^{1}H and ^{13}C). Also, the structures are unambiguously confirmed with X-ray crystallographic analysis.

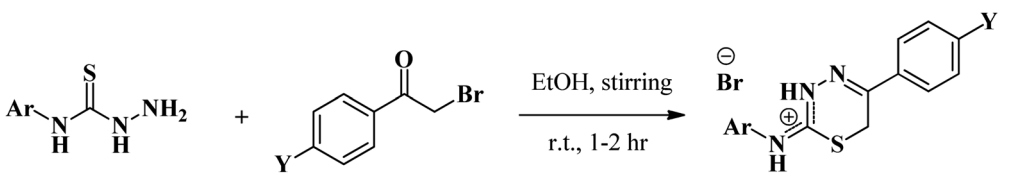

8a-e

8a, Ar = Ph
8b, Ar = Et
8c, Ar = Allyl
8d, Ar = Cyclohexyl
8e, Ar = Me

2a,b

2a, Y = H
2b, Y = Br

9a-g

9a, Ar = Ph, Y = H
9b, Ar = Allyl, Y = H
9c, Ar = Cyclohexyl, Y = H
9d, Ar = Ph, Y = Br
9e, Ar = Me, Y = Br
9f, Ar = Et, Y = Br
9g, Ar = Cyclohexyl, Y = Br

9a, 1 hr (95%); **9b**, 2 hr (91%); **9c**, 1.30 hr (86%); **9d**, 1 hr (87%); **9e**, 1.45 hr (78%); **9f**, 1.50 hr (78%); **9g**, 1.20 hr (81%)

Scheme 2 Synthesis of 1,3,4-thiadiazin-3-ium bromide derivatives **9a–g**.

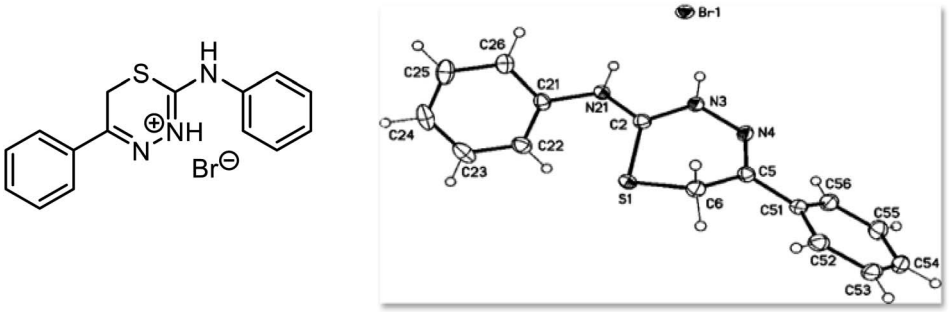

Fig. 2 X-ray crystal structure of compound **9a** (5-phenyl-2-(phenylamino)-6*H*-1,3,4-thiadiazin-3-ium bromide) (displacement parameters are drawn at 50% probability level).

To illustrate our obtained products, we chose compound **9a** (Fig. 2) as an example, which was assigned as 5-phenyl-2-(phenylamino)-6*H*-1,3,4-thiadiazin-3-ium bromide. In the IR spectrum of compound **9a**, broad bands were observed at 3164 cm^{-1} due to NH 3015 cm^{-1} because of aromatic-CH—the other two peaks at 1617 and 1594 cm^{-1} due to C=N and C=C, respectively. Also, the ^{1}H NMR spectra of **9a** showed three broad singlet signals at δ_H = 3.91, 9.45, and 12.85 ppm, which were assigned as 1,3,4-thiadizinium-CH_2,[56] exocyclic-NH and 1,3,4-thiadizinium-NH^+, respectively. The two NH-protons show a downfield shift, attributed to the high deshielding caused by the positive charge on 1,3,4-thiadizinium-ringas observed from the X-ray structure analysis of **9a** (Fig. 2); furthermore, in ^{13}C NMR spectrum of **9a** signals at 23.26, 144.32, and 150.71 ppm, which were assigned as CH_2, thiadiazinium-C5 and thiadiazinium-C2, respectively, in addition to aromatic carbons. Through the preceding data and X-rays displayed in Fig. 2 and 3, we do not doubt that the structures for our obtained products are confirmed.

Furthermore, the NMR of compound **9b**, also known as (*Z*)-*N*-(5-phenyl-3,6-dihydro-2*H*-1,3,4-thiadiazin-2-ylidene)prop-2-en-1-aminium bromide. The ^{1}H NMR spectrum revealed two downfield shifts at δ 12.98 and 10.62 ppm, corresponding to cyclic-NH and exocyclic-NH^+. The allylic protons appeared at δ_H = 4.01–4.04 ppm as triplet with two protons for allyl-CH_2, at 5.23–5.34 ppm, as doublet of doublet (dd) with two protons for allyl-CH_2= and multiplet signal with one proton at δ_H = 5.72–5.83 ppm, for the allylic-CH=, in addition to singlet signal with upfield chemical shift at δ_H = 4.10 ppm, which assigned as CH_2-group. The inverted values of the cyclic and exocyclic-NH's in both compounds **9a** and **9b** are owing to the delocalization of the positive charge over the cyclic-N and amino-nitrogen (exocyclic-N), as well as the hydrogen bond between the nitrogen atoms-H and bromine.

The mass spectra of both **9a** and **9b** compounds revealed molecular ion peaks (M^+) at 347 and 311 *m*/*z*, confirming that the products are formed as a result of the reaction between phenacyl bromide and 4-phenyl/allyl thiosemicarbazide, with the elimination of an H_2O molecule and another HBr molecule. Moreover, the structure of **9b** was confirmed by X-ray crystallography, as illustrated in Fig. 3.

The X-ray structure of compound **9b** confirms the loss of one molecule of H_2O, and the HBr molecule adheres to the crystallite, as indicated in the mass fragmentation pattern of compound **9b** in Fig. 4.

Furthermore, X-ray crystallographic studies validated the structure of all obtained products, as clarified by the crystallographic data of compounds **9a** and **9b** (note that the

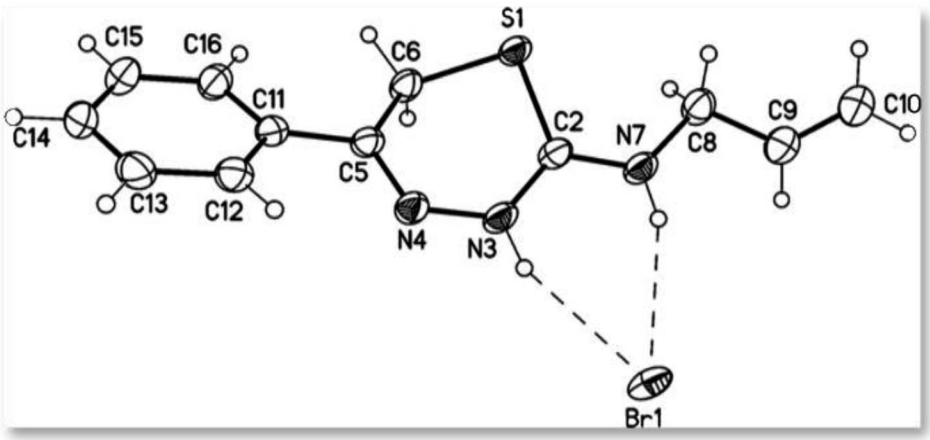

Fig. 3 X-ray crystal structure of compound **9b** ((*Z*)-*N*-(5-phenyl-3,6-dihydro-2*H*-1,3,4-thiadiazin-2-ylidene)prop-2-en-1-aminium bromide) (displacement parameters are drawn at 50% probability level).

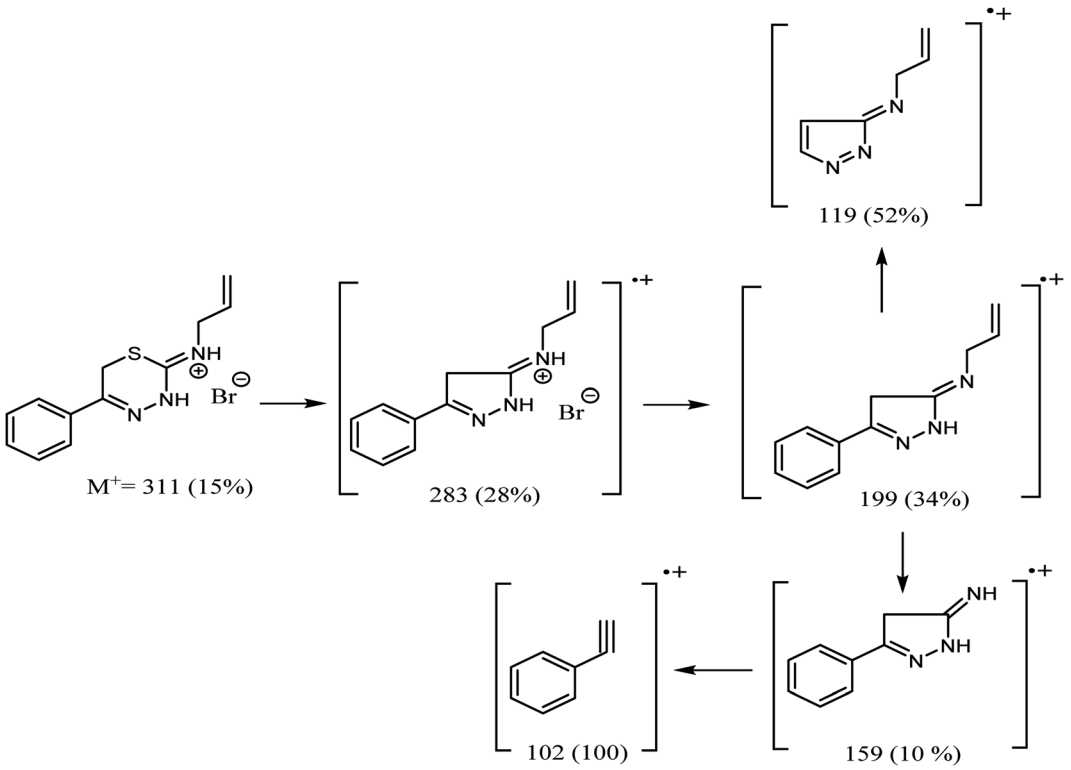

Fig. 4 Fragmentation pattern of compound **9b**.

crystallographic numbering does not mirror the systematic IUPAC numbering) (Fig. 2 and 3). The X-ray data of **9a** revealed that its molecular formula is $C_{15}H_{14}N_3S\cdot Br$ with a weight of m/z = 348.26, a colorless crystal, and a monoclinic shape with space group $P2_1/n$. The measured bond lengths of S1–C2 and S1–C6 bond length are 1.7304 (14) and 1.8148 (19) Å, respectively, are slightly different from the S–C single bond of 1.737 Å, and this is attributed to the sp^2 character of C2 and the sp^3 character of C6. The bond lengths of C2–N3 and C2–N7 are equal to 1.3346 (18) Å, and 1.3259 (19) Å showed some double bond character as they are comparable to the C–N σ-bond length of 1.47 Å and this confirmed the delocalization of the double bond as well as the positive charge. In contrast, the X-ray data of compound **9b** showed that the crystal has an orthorhombic shape with space group *pbca*. It is observed from the bond length table of compound **9b** that the S1–C2 and S1–C6 bond lengths are 1.7290 (15) and 1.8034 (16) Å, respectively, are slightly different from the S–C single bond of 1.737 Å and this is attributed to the sp^2 character of C2 and the sp^3 character of C6. The bond lengths of C2–N3 (1.331 (2)) Å and C2–N7 (1.316 (2)) Å suggest that these bonds have some double bond character as they are comparable to the C–N σ-bond length of 1.47 Å, the N3–N4 bond length is 1.3954(18) Å is closed to the N–N single bond 1.401 Å. Observing the mentioned values of bond lengths confirms the presence of a positive charge, which makes the bond length longer.

The suggested mechanism for forming thiadiazin-3-ium bromides **9a–g** derivatives is as depicted in Scheme 3. Initially, a nucleophilic attack from the NH_2 group to the carbonyl group and condensation occurs with a loss of H_2O molecule. After that, inter-nucleophilic occurs *via* S-atom (S_N2 reaction *S*-alkylation step) on the methylene group, and cyclization takes place, resulting in the formation of the salt 12 which undergoes rearrangement and forming 2-amino-1,3,4-thiadiazinium bromide derivatives **8a–g**.

3.2. Biology

3.2.1. Cell viability assay. To test the viability impact of new targets **9a–g**, the human mammary gland epithelial (MCF-10A) normal cell line was used.[46,47] The cell viability of **9a–g** was determined using the MTT test after four days of incubation on MCF-10A cells. Table 1 indicates that none of the compounds examined were cytotoxic, and all derivatives showed more than 88% cell viability at 50 μM.

3.2.2. Antiproliferative activity. The MTT assay[5,48] was used to investigate the antiproliferative efficacy of targets **9a–g** against four human cancer cell lines: lung cancer (A-549) cell line, colon cancer (HT-29), pancreatic cancer (Panc-1) cell line, and breast cancer (MCF-7) cell line. Erlotinib was used as a reference. Table 1 shows each compound's median inhibitory concentration (IC50) and average inhibitory concentration (GI50) against the four cancer cell lines.

In general, targets **9a–g** displayed good antiproliferative activity, with GI_{50} ranging from 38 nM to 66 nM against the four cancer cell lines, when compared to the reference Erlotinib (GI_{50} = 33 nM), and all examined compounds demonstrated less potent efficacy than Erlotinib. Compounds **9a**, **9c**, and **9d**

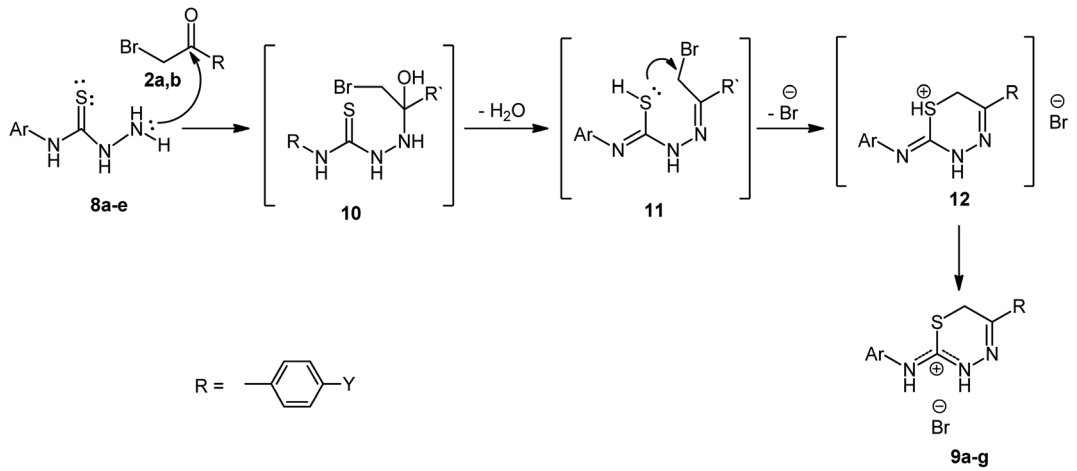

Scheme 3 Suggested mechanism for the formation of 2-amino-1,3,4-thiadiazinium bromide derivatives **9a–g**.

Table 1 IC_{50} values of compounds **9a–g** against four cancer cell lines

		Antiproliferative activity $IC_{50} \pm SEM$ (nM)				
Comp.	Cell viability%	A-549	MCF-7	Panc-1	HT-29	Average (GI_{50})
9a	91	43 ± 4	40 ± 4	44 ± 4	44 ± 4	43
9b	90	56 ± 5	52 ± 5	58 ± 5	58 ± 5	56
9c	92	37 ± 3	35 ± 3	38 ± 3	40 ± 4	38
9d	89	48 ± 4	44 ± 4	48 ± 4	47 ± 4	47
9e	92	62 ± 6	58 ± 5	64 ± 6	64 ± 6	62
9f	89	65 ± 6	64 ± 6	66 ± 6	66 ± 6	66
9g	88	54 ± 5	51 ± 5	56 ± 5	56 ± 5	54
Erlotinib	ND	30 ± 3	40 ± 3	30 ± 3	30 ± 3	33

were the most potent antiproliferative derivatives, with GI_{50} values of 43, 38, and 47 nM, respectively.

Compound **9c** (Ar = cyclohexyl, Y = H) was the most potent derivative of all developed compounds, with a GI_{50} value of 38 nM, and was more effective than Erlotinib against the MCF-7 cancer cell line, with an IC_{50} value of 35 nM *versus* Erlotinib's IC_{50} value of 40 nM. The replacement of the cyclohexyl group in the thiadiazine moiety with a phenyl group, as in compound **9a** (Ar = Ph, Y = H), or with an allyl group, as in compound **9b** (Ar = Allyl, Y = H), resulting in a reported decrease in antiproliferative activity. Compounds **9a** and **9b** had GI_{50} values of 43 and 56 nM, respectively, which were 1.2- and 1.5-fold lower than **9c**, suggesting that the cyclohexyl group at position 2 of the thiadiazine moiety is better tolerated for antiproliferative action than the phenyl and allyl groups.

Moreover, the substitution pattern of the phenyl group at position 5 of the thiadiazine moiety might greatly influence the antiproliferative activity of these molecules. For instance, the 4-bromo derivative **9g** (Ar = cyclohexyl, Y = Br) was less effective than the unsubstituted derivative **9c** (Ar = cyclohexyl, Y = H). Compound **9g** exhibited a GI_{50} value of 54 nM, suggesting that substituting a bromine atom in the *para*-position of the phenyl group is not beneficial for its activity. The same holds when comparing compound **9a** (Ar = Ph, Y = H) with compound **9d** (Ar = Ph, Y = Br). It was found that compound **9a** had a GI_{50} value of 43 nM, but compound **9d** had a GI_{50} value of 47 nM.

Finally, compounds **9e** (Ar = Me, Y = Br) and **9f** (Ar = Et, Y = Br) were the least effective, with GI_{50} values of 62 and 66 nM, respectively. This suggests that having methyl and ethyl groups at position 2 of the thiadiazine moiety is not beneficial for activity.

3.2.3. EGFR inhibitory assay. The EGFR-TK test[49,50] was conducted to assess the inhibitory strength of the most potent antiproliferative derivatives **9a**, **9c**, and **9d** against EGFR, and the results are detailed in Table 2. The assay results align with the antiproliferative assay, showing that the most effective derivatives of EGFR inhibitors were compounds **9a** (Ar = Ph, Y = H), **9c** (Ar = cyclohexyl, Y = H), and **9d** (Ar = Ph, Y = Br) with IC_{50} values of 92 ± 7, 86 ± 5 nM, and 96 ± 7, respectively. The studied compounds were consistently less effective as EGFR inhibitors than the reference Erlotinib, which has an IC_{50} value of 80 nM, Table 2. Compound **9c** (Ar = cyclohexyl, Y = H) exhibited notable anti-EGFR effects, with an IC_{50} value of 86 ± 6 nM, comparable to Erlotinib. On the other hand, compounds **9a** (Ar = Ph, Y = H) and **9d** (Ar = Ph, Y = Br) demonstrated moderate EGFR inhibition, with IC_{50} values of 92 ± 7 and 96 ± 7 nM, respectively. The data suggest that compound **9c** has potential as an EGFR inhibitor and could be used as a candidate for antiproliferative purposes.

3.2.4. $BRAF^{V600E}$ inhibitory assay. *In vitro* testing assessed the anti-$BRAF^{V600E}$ activity of compounds **9a**, **9c**, and **9d**.[51,52] The enzyme testing showed that the examined derivatives moderately hindered $BRAF^{V600E}$, with IC_{50} values varying from 74 to 88 nM, as indicated in Table 2. The IC_{50} values of the compounds studied are higher than those of the reference drugs Erlotinib (IC_{50} = 60 nM) and Vemurafenib (IC_{50} = 30 nM). Compound **9c** had the highest inhibitory action against $BRAF^{V600E}$ with an IC_{50} of 74 nM and was identified as a potential inhibitor of cancer cell proliferation with a GI_{50} of 38 nM. Consequently, compound **9c** becomes a potential antiproliferative agent that functions as a dual inhibitor of EGFR and $BRAF^{V600E}$. On the other hand, additional structural

Table 2 IC_{50} values of compounds **9a**, **9c**, and **9d** against EGFR, and $BRAF^{V600E}$

Compound	EGFR inhibition $IC_{50} \pm$ SEM (nM)	$BRAF^{V600E}$ inhibition $IC_{50} \pm$ SEM (nM)	VEGFR-2 inhibition $IC_{50} \pm$ SEM (nM)
9a	92 ± 7	83 ± 6	2.80 ± 0.02
9c	86 ± 6	74 ± 5	2.20 ± 0.02
9d	96 ± 7	88 ± 6	3.25 ± 0.03
Erlotinib	80 ± 5	60 ± 5	ND
Vemurafenib	ND	30 ± 3	ND
Sorafenib	ND	ND	0.17 ± 0.01

modifications might be necessary to successfully obtain more potent lead molecules to develop future cancer therapies.

3.2.5. VEGFR-2 inhibitory assay. The inhibitory potency of compounds **9a**, **9c**, and **9d** against VEGFR-2 was assessed using kinase-glo-luminescent kinase assays,[53] with Sorafenib as the reference drug. Table 2 presents the results in the form of IC_{50} values. The results indicated that compounds **9a**, **9c**, and **9d** showed moderate inhibitory activity against VEGFR-2. Their respective IC_{50} values were 2.80 ± 0.02 nM, 2.20 ± 0.02 nM, and 3.25 ± 0.03 nM. In comparison, Sorafenib exhibited a lower IC_{50} value of 0.17 ± 0.01 nM. All the studied compounds were at least 13-fold less potent than the reference Sorafenib. Once again, compound **9c** had the highest potency as a VEGFR-2 inhibitor, with an IC_{50} value of 2.20 ± 0.02 nM. The results from the *in vitro* experiments indicate that compounds **9a**, **9c**, and **9d** exhibited significant antiproliferative activity and have the potential to function as multitargeted inhibitors.

Table 3 Western blotting analysis of compound **9c** against EGFR, VEGFR-2, and $BRAF^{V600E}$

	Compound			Western blotting OD			
S	Code	MW	Cells	EGFR	VEGFR-2	$BRAF^{V600E}$	β-Actin
1	**9c**	354.31	A549	0.288	0.346	0.219	√
2	Control	—	A549	0.695	0.662	0.507	√

3.3. Western blot analysis

Based on previous results, compound **9c** is highly effective at inhibiting EGFR, $BRAF^{V600E}$, and VEGFR-2, significantly suppressing cell proliferation. The western blotting analysis[54] aids in elucidating the probable mechanisms behind the observed antiproliferative activity of **9c**. The findings of the western blotting analysis agreed with the data obtained from the *in vitro* assays for EGFR, $BRAF^{V600E}$, and VEGFR-2 inhibition. Compound **9c** exhibited a significant decrease in the levels of the specific enzymes, with inhibition percentages ranging from 47% to 58% when compared to the positive control A549 untreated cells (as shown in Table 3 and Fig. 5). The findings of this study confirm the outcomes of the *in vitro* experiment, demonstrating that compound **9c** exerts its antiproliferative effects *via* multitargeted inhibitory action.

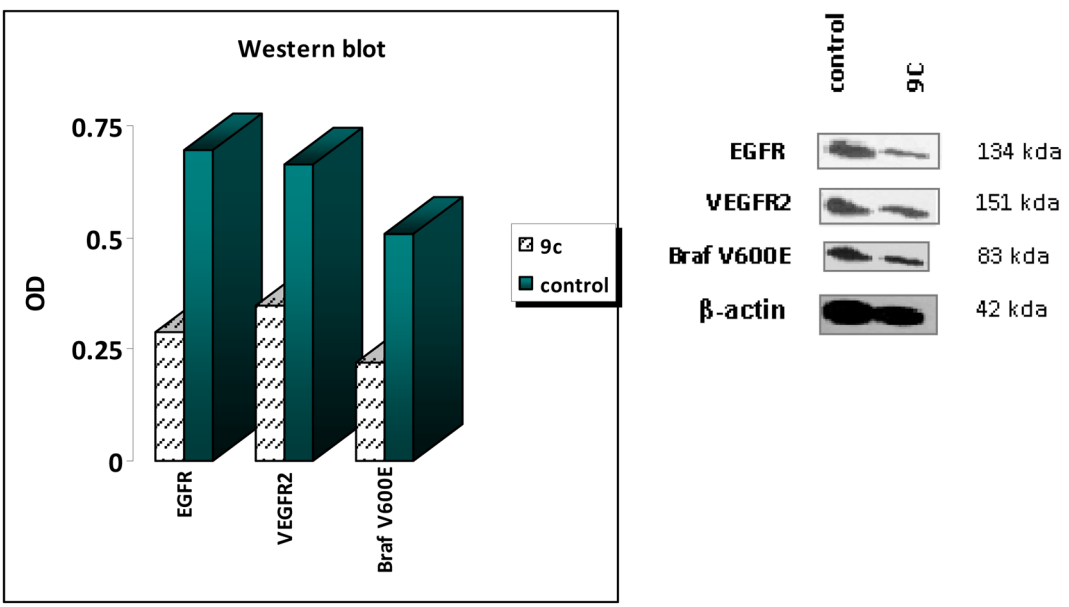

Fig. 5 Results of western blotting of compound **9c** against EGFR, VEGFR-2, and $BRAF^{V600E}$.

4. Conclusion

This study discusses the preparation of thiadiazines heterocycle **9a–g** through the reaction between 4-substituted thiosemicarbazides and α-halo ketones. The accurate structure was established and verified by X-ray diffraction analysis. A comparison was conducted, revealing contradictory findings in other scholarly works. Compounds **9a–g** were investigated as EGFR, $BRAF^{V600E}$, and VEGFR-2 inhibitors in quest of a multi-targeted antiproliferative scaffold. The results showed that compound **9c** is a promising antiproliferative agent inhibiting EGFR, $BRAF^{V600E}$, and VEGFR-2. On the other hand, further structural modifications may be required to successfully acquire more potent lead compounds to develop future cancer medicines.

Sample availability

Samples of compounds **9a–g** are available from the authors.

Author contributions

Bahaa G. M. Youssif, Essmat M. El-Sheref, and Hendawy N. Tawfeek: conceptualization, methodology, writing, editing and revision. Alshaimaa Abdelmoez and Kholood Dahlous: writing, editing and revision. S. Bräse: writing and editing. Kari Rissanen, M. Nieger: X-ray analysis.

Conflicts of interest

The authors state that they do not have any known competing financial interests or personal links that could appear to have influenced the work disclosed in this study.

Acknowledgements

This work was funded by the Researchers Supporting Project Number (RSP2024R388) at King Saud University, Riyadh, Saudi Arabia. The authors also acknowledge support from the KIT-Publication Fund of the Karlsruhe Institute of Technology.

References

1 W. Cao, H.-D. Chen, Y.-W. Yu, N. Li and W.-Q. Chen, *Chinese Med. J.*, 2021, **134**, 783–791.
2 K. El-Adl, H. M. Sakr, R. G. Yousef, A. B. Mehany, A. M. Metwaly, M. A. Elhendawy, M. M. Radwan, M. A. ElSohly, H. S. Abulkhair and I. H. Eissa, *Bioorg. Chem.*, 2021, **114**, 105105.
3 A. S. Correia, F. Gärtner and N. Vale, *Heliyon*, 2021, **7**(1), e05948.
4 R. A. Mekheimer, S. M. Allam, M. A. Al-Sheikh, M. S. Moustafa, S. M. Al-Mousawi, Y. A. Mostafa, B. G. Youssif, H. A. Gomaa, A. M. Hayallah and M. Abdelaziz, *Bioorg. Chem.*, 2022, **121**, 105693.
5 M. A. Mahmoud, A. F. Mohammed, O. I. Salem, S. M. Rabea and B. G. Youssif, *J. Mol. Struct.*, 2023, **1282**, 135165.
6 F. O. A. Frejat, H. Zhai, Y. Cao, L. Wang, Y. A. Mostafa, H. A. Gomaa, B. G. Youssif and C. Wu, *Bioorg. Chem.*, 2022, **126**, 105922.
7 L. H. Al-Wahaibi, M. A. Mahmoud, Y. A. Mostafa, A. E. Raslan and B. G. Youssif, *J. Enzyme Inhib. Med. Chem.*, 2023, **38**, 376–386.
8 L. N. Puls, M. Eadens and W. Messersmith, *Oncologist*, 2011, **16**, 566–578.
9 A. D. Boran and R. Iyengar, *Current Opinion in Drug Discovery & Development*, 2010, vol. 13, p. 297.
10 J. J. Frost, *Int. J. Unconv. Comput.*, 2021, **16**, 41–78.
11 D. C. Altieri, *Future Oncol.*, 2010, **6**, 487–489.
12 K. Paraiso, I. Fedorenko, L. Cantini, A. Munko, M. Hall, V. Sondak, J. Messina, K. Flaherty and K. Smalley, *Br. J. Cancer*, 2010, **102**, 1724–1730.
13 K. T. Flaherty, J. R. Infante, A. Daud, R. Gonzalez, R. F. Kefford, J. Sosman, O. Hamid, L. Schuchter, J. Cebon and N. Ibrahim, *N. Engl. J. Med.*, 2012, **367**, 1694–1703.
14 G. V. Long, D. Stroyakovskiy, H. Gogas, E. Levchenko, F. de Braud, J. Larkin, C. Garbe, T. Jouary, A. Hauschild and J. J. Grob, *N. Engl. J. Med.*, 2014, **371**, 1877–1888.
15 C. Robert, B. Karaszewska, J. Schachter, P. Rutkowski, A. Mackiewicz, D. Stroiakovski, M. Lichinitser, R. Dummer, F. Grange and L. Mortier, *N. Engl. J. Med.*, 2015, **372**, 30–39.
16 A. Ribas, R. Gonzalez, A. Pavlick, O. Hamid, T. F. Gajewski, A. Daud, L. Flaherty, T. Logan, B. Chmielowski and K. Lewis, *Lancet Oncol.*, 2014, **15**, 954–965.
17 R. S. Finn, M. Martin, H. S. Rugo, S. Jones, S.-A. Im, K. Gelmon, N. Harbeck, O. N. Lipatov, J. M. Walshe and S. Moulder, *N. Engl. J. Med.*, 2016, **375**, 1925–1936.
18 C. T. Keith, A. A. Borisy and B. R. Stockwell, *Nat. Rev. Drug Discov.*, 2005, **4**, 71–78.
19 L. H. Al-Wahaibi, A. F. Mohammed, F. E.-Z. S. Abdel Rahman, M. H. Abdelrahman, X. Gu, L. Trembleau and B. G. Youssif, *J. Enzym. Inhib. Med. Chem.*, 2023, **38**, 2218602.
20 L. H. Al-Wahaibi, A. F. Mohammed, M. H. Abdelrahman, L. Trembleau and B. G. Youssif, *Pharmaceuticals*, 2023, **16**, 1039.
21 US Department of Health and Human Services, *Nutr. Today*, 1990, **25**(6), 29–39.
22 A. A. Mourad, Y. W. Rizzk, I. Zaki, F. Z. Mohammed and M. El Behery, *J. Mol. Struct.*, 2021, **1242**, 130722.
23 A. Ahmad, H. Varshney, A. Rauf, A. Sherwani and M. Owais, *Arab. J. Chem.*, 2017, **10**, S3347–S3357.
24 A. Anant, A. Ali, A. Ali, G. Gupta and V. Asati, *J. Mol. Struct.*, 2021, **1245**, 131079.
25 S. H. Ali and A. R. Sayed, *Synth. Commun.*, 2021, **51**, 670–700.
26 A. A. Abu-Hashem, A.-R. El-Gazzar, H. N. Hafez, A. A. M. Abdelgawad and M. A. Gouda, *Mini-Rev. Org. Chem.*, 2024, **21**, 151–171.
27 F. A. Ragab, S. A. Abdel-Aziz, M. Kamel, A. M. A. Ouf and H. A. Allam, *Bioorg. Chem.*, 2019, **93**, 103323.
28 B. Zhang, Y.-H. Li, Y. Liu, Y.-R. Chen, E.-S. Pan, W.-W. You and P.-L. Zhao, *Eur. J. Med. Chem.*, 2015, **103**, 335–342.
29 M. I. Ismail, S. Mohamady, N. Samir and K. A. Abouzid, *ACS Omega*, 2020, **5**, 20170–20186.

30 Q. Xu, K. Bao, M. Sun, J. Xu, Y. Wang, H. Tian, D. Zuo, Q. Guan, Y. Wu and W. Zhang, *Sci. Rep.*, 2017, **7**, 11997.
31 L. Ji, Y. Zhou, Q. Yu, Y. Fang, Y. Jiang, Y. Zhao, C. Yuan and W. Xie, *J. Mol. Struct.*, 2021, **1227**, 129406.
32 R. H. Vekariya, K. D. Patel, N. P. Prajapati and H. D. Patel, *Synth. Commun.*, 2018, **48**, 1505–1533.
33 A. A. Hassan, N. K. Mohamed, A. A. Aly, H. N. Tawfeek, H. Hopf, S. Bräse and M. Nieger, *Mol. Diversity*, 2019, **23**, 821–828.
34 A. A. Hassan, A. A. Aly, M. Ramadan, N. K. Mohamed, H. N. Tawfeek, S. Bräse and M. Nieger, *Monatsh. Chem.*, 2020, **151**, 1453–1466.
35 A. A. Hassan, N. K. Mohamed, A. A. Aly, H. N. Tawfeek, S. Bräse and M. Nieger, *J. Mol. Struct.*, 2019, **1176**, 346–356.
36 H. BoBooth, D. V. Griffiths and M. L. Jozefowicz, *J. Chem. Soc., Perkin Trans. 2*, 1980, 255.
37 W.-D. Pfeiffer, E. Dilk, H. Rossberg and P. Langer, *Synlett*, 2003, **2003**, 2392–2394.
38 W. W. Wardakhan, *Arch. Pharmazie*, 2006, **339**, 608–615.
39 S. Rostamizadeh, A. M. Amani and N. Shadjou, *Phosphorus, Sulfur, Silicon Relat. Elem.s*, 2012, **187**, 238–244.
40 A. A. Aly, E. M. El-Sheref, A. B. Brown, S. Bräse, M. Nieger and E.-S. M. Abdelhafez, *J. Sulfur Chem.*, 2019, **40**, 641–647.
41 W. D. Pfeiffer, D. Junghans, A. S. Saghyan and P. Langer, *J. Heterocycl. Chem.*, 2014, **51**, 1063–1067.
42 B. G. Youssif, A. M. Gouda, A. H. Moustafa, A. A. Abdelhamid, H. A. Gomaa, I. Kamal and A. A. Marzouk, *J. Mol. Struct.*, 2022, **1253**, 132218.
43 H. A. El-Sherief, B. G. Youssif, A. H. Abdelazeem, M. Abdel-Aziz and H. M. Abdel-Rahman, *Anti Cancer Agents Med. Chem.*, 2019, **19**, 697–706.
44 M. B. Alshammari, A. A. Aly, B. G. Youssif, S. Bräse, A. Ahmad, A. B. Brown, M. A. Ibrahim and A. H. Mohamed, *Front. Chem.*, 2022, **10**, 1076383.
45 M. Tišler, *Croat. Chem. Acta*, 1956, **28**, 147–154.
46 A. A. Hassan, N. K. Mohamed, A. A. Aly, M. Ramadan, H. A. Gomaa, A. T. Abdel-Aziz, B. G. Youssif, S. Bräse and O. Fuhr, *Molecules*, 2023, **28**, 7951.
47 A. M. Mohassab, H. A. Hassan, H. A. Abou-Zied, M. Fujita, M. Otsuka, H. A. Gomaa, B. G. Youssif and M. Abdel-Aziz, *J. Mol. Struct.*, 2024, **1297**, 136953.
48 M. A. Mahmoud, A. F. Mohammed, O. I. Salem, T. M. Almutairi, S. Bräse and B. G. Youssif, *J. Enzyme Inhib. Med. Chem.*, 2024, **39**, 2305856.
49 A. A. Aly, M. B. Alshammari, A. Ahmad, H. A. Gomaa, B. G. Youssif, S. Bräse, M. A. Ibrahim and A. H. Mohamed, *Arab. J. Chem.*, 2023, **16**, 104612.
50 L. H. Al-Wahaibi, A. F. Mohammed, M. H. Abdelrahman, L. Trembleau and B. G. Youssif, *Molecules*, 2023, **28**, 1269.
51 L. H. Al-Wahaibi, M. Hisham, H. A. Abou-Zied, H. A. Hassan, B. G. Youssif, S. Bräse, A. M. Hayallah and M. Abdel-Aziz, *Pharmaceuticals*, 2023, **16**, 1522.
52 A. M. Mohassab, H. A. Hassan, D. Abdelhamid, A. M. Gouda, B. G. Youssif, H. Tateishi, M. Fujita, M. Otsuka and M. Abdel-Aziz, *Bioorg. Chem.*, 2021, **106**, 104510.
53 A. A. Marzouk, S. A. Abdel-Aziz, K. S. Abdelrahman, A. S. Wanas, A. M. Gouda, B. G. Youssif and M. Abdel-Aziz, *Bioorg. Chem.*, 2020, **102**, 104090.
54 W. N. Burnette, *Anal. Biochem.*, 1981, **112**, 195–203.
55 A. A. Hassan, N. K. Mohamed, A. A. Aly, H. N. Tawfeek, S. Bräse and M. Nieger, *Monatsh. Chem.*, 2020, **151**, 1143–1152.
56 W. D. Jones Jr, J. M. Kane and A. D. Sill, *J. Heterocycl. Chem.*, 1983, **20**, 1359–1361.